Journal of Solid State Chemistry ∎ (∎∎∎∎) ∎∎∎–∎∎∎

Contents lists available at ScienceDirect

Journal of Solid State Chemistry

journal homepage: www.elsevier.com/locate/jssc

Crystal growth of Bi_2Te_3 and noble cleaved (0001) surface properties

V.V. Atuchin [a,b,*], V.A. Golyashov [c,d], K.A. Kokh [e,f,g], I.V. Korolkov [d,h], A.S. Kozhukhov [d,i], V.N. Kruchinin [j], I.D. Loshkarev [k], L.D. Pokrovsky [a], I.P. Prosvirin [d,l], K.N. Romanyuk [m,n], O.E. Tereshchenko [c,d,g]

[a] Laboratory of Optical Materials and Structures, Institute of Semiconductor Physics, SB RAS, Novosibirsk 630090, Russia
[b] Functional Electronics Laboratory, Tomsk State University, Tomsk 634050, Russia
[c] Laboratory of Molecular Beam Epitaxy of III-V Semiconductors, Institute of Semiconductor Physics, SB RAS, Novosibirsk 630090, Russia
[d] Novosibirsk State University, Novosibirsk 630090, Russia
[e] Laboratory of Crystal Growth, Institute of Geology and Mineralogy, SB RAS, Novosibirsk 630090, Russia
[f] Laboratory of Nanostructured Surfaces, Tomsk State University, Tomsk 634050, Russia
[g] Spintronics Laboratory, Saint Petersburg State University, Saint Petersburg 198504, Russia
[h] Laboratory of Crystal Chemistry, Nikolaev Institute of Inorganic Chemistry, SB RAS, Novosibirsk 630090, Russia
[i] Laboratory of Nanodiagnostics and Nanolithography, Institute of Semiconductor Physics, SB RAS, Novosibirsk 630090, Russia
[j] Laboratory for Ellipsometry of Semiconductor Materials and Structures, Institute of Semiconductor Physics, SB RAS, Novosibirsk 630090, Russia
[k] Laboratory of Molecular Beam Epitaxy of Elementary Semiconductors and A3B5 Compounds, Institute of Semiconductor Physics, SB RAS, Novosibirsk 630090, Russia
[l] Boreskov Institute of Catalysis, SB RAS, Novosibirsk 630090, Russia
[m] Department of Materials and Ceramic Engineering & CICECO, University of Aveiro, 3810-193 Aveiro, Portugal
[n] Institute of Natural Sciences, Ural Federal University, Ekaterinburg 620083, Russia

ARTICLE INFO

Article history:
Received 29 June 2015
Received in revised form
20 July 2015
Accepted 21 July 2015

Keywords:
Bi_2Se_3
Bridgman technique
Cleavage
XRD
RHEED
AFM
STM
SE
XPS

ABSTRACT

A high quality Bi_2Te_3 crystal has been grown by Bridgman method with the use of rotating heat field. The phase purity and bulk structural quality of the crystal have been verified by XRD analysis and rocking curve observation. The atomically smooth Bi_2Te_3(0001) surface with an excellent crystallographic quality is formed by cleavage in the air. The chemical and microstructural properties of the surface have been evaluated with RHEED, AFM, STM, SE and XPS. The Bi_2Te_3(0001) cleaved surface is formed by atomically smooth terraces with the height of the elemental step of $\sim 1.04 \pm 0.1$ nm, as estimated by AFM. There is no surface oxidation process detected over a month keeping in the air at normal conditions, as shown by comparative core level photoelectron spectroscopy.

© 2015 Published by Elsevier Inc.

1. Introduction

Bismuth telluride, Bi_2Te_3, is a representative member of the Bi_2Se_3 crystal family well-known for its pronounced layered crystal structure and good thermoelectric properties [1–5]. Recently, Bi_2Te_3 has become of wide research interest as a three-dimensional topological insulator (TI) where the novel state of quantum matter is realized [6–13]. Such electronic system possesses strong spin-orbit coupling that provides a combination of an insulating bulk and massless Dirac fermion surface states. The experimental realization of TI states was carried out by several methods including thin film and nanoplate preparation [9,10,12,14–16]. Besides this, it is well known that Bi_2Se_3 family crystals possess good cleavage properties and high-quality (0001) surface of macroscopic area can be prepared using the bulk crystal and cleavage procedure [5,7,17–24]. This method of the pristine surface preparation was used in many experiments on TI effect observation and top surface engineering of Bi_2Se_3–family crystals. Regrettably, as a rule, only a very short description of the crystal growth conditions and surface preparation conditions can be found in literature [7,17,18,21–30]. The formation and stability of the TI state at the crystal–vacuum (or air) boundary and device

* Correspondence to: Institute of Semiconductor Physics, 630090 Novosibirsk 90, Russia. Fax: +7 383 3332771.
E-mail address: atuchin@thermo.isp.nsc.ru (V.V. Atuchin).

http://dx.doi.org/10.1016/j.jssc.2015.07.031
0022-4596/© 2015 Published by Elsevier Inc.

structures in particular, however, may be strongly dependent on the structural and chemical qualities of the Bi_2Te_3 crystal and the cleaved surface properties seem to be among governing factors. The present study is aimed at the growth of a high quality Bi_2Te_3 crystal and evaluation of structural and chemical parameters of the cleaved (0001) surface.

Commonly, the surface of telluride compounds is not inert in the air and tends to oxidize due to drastic affinity for oxygen [31–35]. For many complex halcogenide compounds, the chemical interaction with air agents results in a complete decomposition and amorphization that limit the crystal living period. From this point of view, Bi_2Te_3 seems to be not an exception and the presence of oxygen could be expected at the crystal surface. Indeed, oxide presence at the surface of Bi_2Te_3 nanocrystals fabricated by very different techniques was found by XPS in several experiments [36–39]. The behavior of the cleaved Bi_2Te_3(0001) surface is evidently different. The swift oxygen adsorption was detected when the cleaved surface was prepared in the dry nitrogen atmosphere [40]. On the other hand, the Bi_2Te_3(0001) surface cleaved in the air and immediately measured with XPS shows the absence of an oxygen signal [41]. However, the pronounced oxidation was detected even after 4 h keeping in the air atmosphere at $T=24$ °C, and that indicates active chemical interaction of the cleaved Bi_2Te_3(0001) surface with the air agents [41]. It should be pointed that the parallel formation of Bi_2O_3- and TeO_2-type species was found at the surface in this experiment.

Many versions of the Bi–Te equilibrium phase diagram can be found in the literature, and at least one intermetallic phase, Bi_2Te_3, is generally accepted at Bi:Te=1:1 [42–44]. The crystal structure of trigonal Bi_2Te_3, space group R-3 m, $a=4.3896$ and $b=30.5090$ Å, $Z=3$, is shown in Fig. 1 [45,46]. The crystal lattice is formed by the bilayers of face-sharing $BiTe_6$ octahedrons (quintuple). The bilayers are stacked along the c axis by weak van der Waals bonds with as long Te–Te distance as 364 pm. This layered structure provides excellent cleavage properties of Bi_2Te_3 and other members of the Bi_2Se_3 crystal family. On cleavage, the long interlayer Te–Te bonds are disrupted and the (0001) surface is supposed to be Te-terminated. In addition, it should be noted that the phase transition of Bi_2Te_3 into the Bi_2Te_3 II modification, R-3m, $a=4.417$ and $b=29.84$ Å, $Z=3$, was found at a higher temperature and pressure [47]. This orthorhombic modification is metastable under normal conditions. Other properties of the Bi_2Se_3 II phase are unknown.

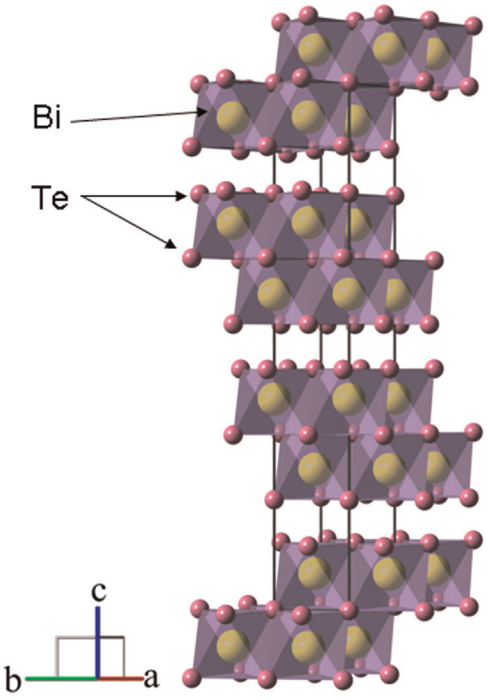

Fig. 1. The crystal structure of Bi_2Te_3. The unit cell is outlined. The lone atoms are omitted for clarity.

2. Experimental

Bi_2Te_3 melts congruently at $T=586$ °C forming eutectic in the Te-rich part of the Bi–Te system [42–44]. The Bi-rich part of the diagram is more complicated consisting of a series of peritectic reactions that is very similar to the behavior of the Bi-Se system [48]. Because of active Bi–Te melt oxidation in the air atmosphere, the crystal growth should be carried out in evacuated quartz ampoules. A vapor pressure of the Bi and Te elementary components at the Bi_2Te_3 melting temperature is far lower than the ampoule resistance threshold (~15 kbar), and the charge may be obtained by direct alloying of the components.

In the present work, the charge prepared from elementary Bi (5 N) and Te (4 N) at stoichiometric composition Bi_2Te_3 was sealed into the quartz ampoule evacuated to $\sim 10^{-4}$ Torr. High-purity bismuth was prepared in NIIC (Novosibirsk, Russia) [49]. The mixture heated up to 20 °C above the melting temperature was left for 1 day for homogenization. Then, after cooling, the synthesized polycrystalline ingot was reloaded to the growth quartz ampoule with a conical tip for recrystallization by the modified vertical Bridgman method with a rotating heat field [50,51]. The ampoule translation rate and axial temperature gradient were 10 mm/day and ~15 °C/cm, correspondingly. The rotating heat field parameters were the same as those earlier used for the $AgGaS_2$ crystal growth [51]. The seed technique was not used. However, the conical ampoule tip resulted in the geometrical selection of the single grain at the initial growth stages. The crystallographic orientation of the grain was (0001) plane nearly along the growth axis that is a common feature of layered chalcogenide crystals [19,52–55].

The phase compositions of both synthesized and recrystallized Bi_2Te_3 were evaluated by X-ray diffraction (XRD) analysis. The XRD patterns were recorded using Shimadzu XRD-7000 (Cu Kα radiation, Ni – filter, 5–60° 2θ range) device. The polycrystalline or single-crystal samples were gently ground with hexane in an agate mortar and the resulting suspension was deposited on the polished side of a standard fused-quartz sample holder, a smooth thin layer being formed after drying. The indexing of the diffraction patterns was carried out using the known structural data [45].

The Bi_2Te_3(0001) substrates with the typical dimensions of $8\times10\times1$ mm^3 were prepared by cleaving the crystal with a steel knife in the air atmosphere. The structural quality of the crystal bulk was estimated by the rocking curve measurements. The X-ray rocking curves were recorded using a two-crystal diffractometer DSO-1T ($Cu_{K\alpha1}$ radiation, $\lambda=1.54056$ Å, Ω–2θ scanning, detector aperture is 170 s of arc) equipped with the Ge(004) monochromator [56]. The top-surface crystallographic properties were evaluated with RHEED using an EFZ4 device under electron energy 50 keV [56–58]. RHEED observation was produced during an hour after crystal cleavage. The surface micromorphology of Bi_2Te_3(0001) substrates was studied by AFM with Solver P-47H device in the noncontact mode [26,59]. The STM images and profile measurements were made at room temperature in an UHV chamber with base pressure $\sim 1\times10^{-10}$ Torr with a Omicron scanning tunneling microscope (STM) on the Bi_2Te_3(0001) samples prepared by cleavage [26,60].

The electronic properties of the Bi_2Te_3(0001) surface were characterized by X-ray photoelectron spectroscopy (XPS). The XPS

Please cite this article as: V.V. Atuchin, et al., J. Solid State Chem. (2015), http://dx.doi.org/10.1016/j.jssc.2015.07.031

valence-band and core-level spectra of Bi_2Te_3 were measured using the UHV-Analysis-System assembled by SPECS (Germany). The system is equipped with a PHOIBOS 150 hemispherical analyzer. The base pressure of a sublimation ion-pumped chamber of the system was less than 6×10^{-10} mbar during the present experiments. The Al Kα radiation ($E=1486.6$ eV) was used as a source of XPS spectra excitation. The XPS spectra were recorded at the constant pass energy of 10 eV. The energy scale of the spectrometer was calibrated by setting the measured Au $4f_{7/2}$ and Cu $2p_{3/2}$ binding energies (BE) to 84.00 ± 0.05 eV and 932.66 ± 0.05 eV, respectively, with respect to the Fermi energy, E_F. The energy drift due to charging effects was not detected due to a noticeable bulk conductivity of the Bi_2Te_3 samples. For the peak fitting procedure, a mixture of Lorenzian and Gaussian functions were used together with the Shirley background subtraction method. The details of the sample preparation and measurements can be found elsewhere [19,26,61]. To determine the chemical composition of the Bi_2Te_3 surface, the atomic sensitivity factors (ASF) were initially obtained using pure polycrystalline Bi and Te samples. To remove surface contaminations appeared due to interaction with air, a bombardment of the metal sample surface has been implemented by Ar^+ ions with the energy of 1.05 keV (3–4 μA) up to the exhausting O 1 s photoemission signal.

The spectral dependencies of refractive index $n(\lambda)$ and extinction coefficient $k(\lambda)$ were determined by means of spectroscopic ellipsometry (SE). Ellipsometric angles Ψ and Δ were measured as a function of λ in the spectral range of ~250–1030 nm using an ELLIPS-1771 SA ellipsometer [62]. The instrumental spectral resolution was 2 nm. The recording time of a spectrum did not exceed 20 s and the incidence angle of light beam on the sample was 70°. We used the four-zone method of measuring with subsequent averaging over all the four zones. Ellipsometry parameters Ψ and Δ are related to the complex Fresnel reflection coefficients by the equation

$$tg\Psi\cdot e^{i\Delta}=\frac{R_p}{R_s},$$

where R_p and R_s are the coefficients for the p- and s-polarized lightwaves. To calculate the dependencies of refractive index $n(\lambda)$ and extinction coefficient $k(\lambda)$ on optical wavelength λ, the experimental data were processed using the model of the air-homogeneous isotropic substrate.

3. Results and discussion

As a result, the single metalescent crystal of 10 mm in diameter and 50 mm long was grown, as shown in Fig. 2. The exclusive presence of the pure Bi_2Te_3 phase is confirmed for the as-synthesized sample and the crystal grown. No indication of any foreign phase, including known Bi-reached bismuth tellurides and high-temperature Bi_2Te_3 II, was detected in the XRD pattern, as shown in Fig. 3. At the pattern, the low-intensity halo at $2\theta\sim17$–26° appeared from the amorphous fused-quartz sample holder. The difference between the experimental and theoretical curves is explained by the (000l) preferred orientation of particles prepared by the crystal ground procedure. The bulk structural quality can be estimated by the rocking curve measurement, as shown in Fig. 4. The full width at a half maximum (FWHM) of the (00015) reflex recorded from cleaved crystal plate is ~75″. The RHEED pattern recorded from a cleaved crystal surface is shown in Fig. 5. The superposition of wide Kikuchi lines and crystal reflexes is evident, and that verifies an excellent surface structural quality. There is no amorphous component detected at the cleaved surface that is similar to the cleaved surface structural quality previously observed in the layered crystals of GaSe, Pb_2MoO_5 and AWO_4 (A=Zn, Cd) wolframite-type tungstates without additional surface treatments [55–57,63–65].

As it was shown by AFM observation, the cleaved $Bi_2Te_3(0001)$ surface is formed by atomically smooth terraces with as low rms parameter as ~0.06 nm for the area of 5×5 μm^2. The typical AFM pattern recorded for the field of 5×5 μm^2 with terraces is shown in Fig. 6. A system of several flat terraces is detected for this field. However, contrary to the previous results obtained for the GaSe and $Bi_2Se_3(0001)$ cleaved surface, the large area terraces were not found at the $Be_2Te_3(0001)$ surface [55,66]. Also, it should be pointed that the scattered mesoscale structural defects, previously

Fig. 2. A Bi_2Te_3 crystal grown by the modified vertical Bridgman method with a rotating heat field.

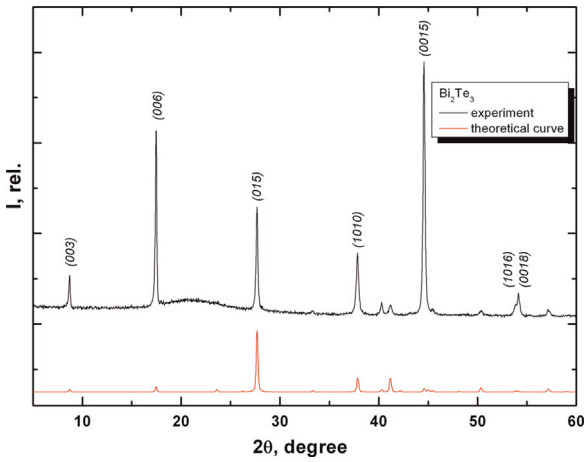

Fig. 3. The experimental and theoretical XRD patterns. The Miller indices of the most intensive lines are depicted.

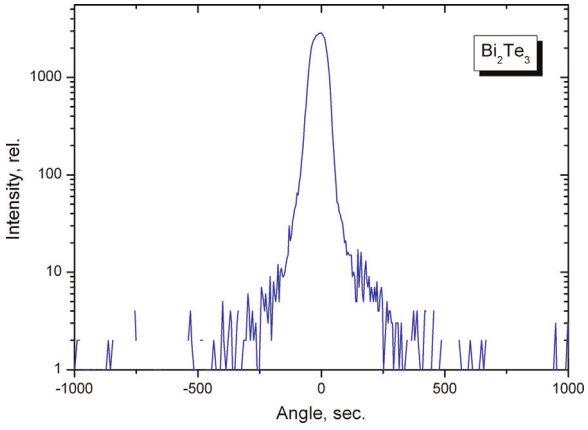

Fig. 4. The rocking curve recorded for reflex (00015) from the cleaved $Bi_2Te_3(0001)$ substrate.

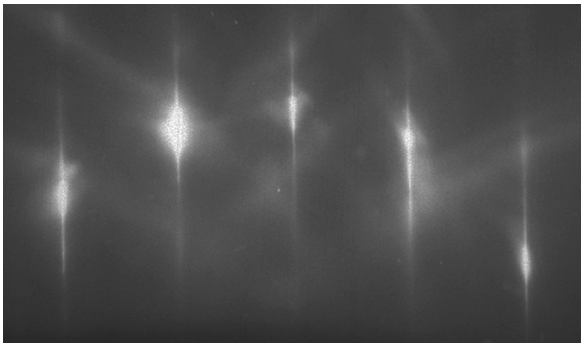

Fig. 5. A Kikuchi lines pattern recorded by RHEED for the cleaved Bi_2Te_3(0001) surface.

observed at the Bi_2Se_3(0001) cleaved surface, were not frequent at the Bi_2Te_3(0001) cleaved surface. At the Bi_2Te_3(0001) surface, the height of the elemental step was estimated by AFM as $\sim 1.04 \pm 0.1$ nm and that is close to the value of $c/3 = 1.05$ nm of Bi_2Te_3[45]. The terrace surface roughness is not above 0.1 nm, as carried out for the fresh cleaved surface. Thus, similar to the Bi_2Se_3(0001) cleaved surface, the Bi_2Te_3(0001) surface is formed by atomically smooth terraces.

The results of STM measurements are shown in Fig. 7. The pattern shown in Fig. 7(a) was recorded from fresh cleaved surface, and the exposure to the air before the sample insertion into the vacuum chamber was at the level of ~30 min. The Bi_2Te_3(0001) surface is atomically clean and is presented by non-reconstructed Te-terminated surface structure 1×1 with the period of ~0.43 nm, as it is evident from Fig. 7(b). This pattern may reveal a comparatively low structural defects density in the Bi_2Te_3 crystal and low ability of the cleaved surface for the adsorption of atmospheric agents.

The dispersive optical constants of Bi_2Te_3 are shown in Fig. 8. The curves were derived using a simple model of (air) – (homogeneous isotropic infinite substrate) without an account of any interface layers, possible surface roughness and other factors affecting ellipsometric angles. The details of the algorithm used for calculations can be found elsewhere [53,67,68]. In the framework of the model, optical parameters n and k can be calculated analytically for each wavelength. Generally, a continuous increase of n and k over the spectral range of 300–1000 nm is observed in Bi_2Te_3. The very high n and k values are achieved at ~1000 nm,

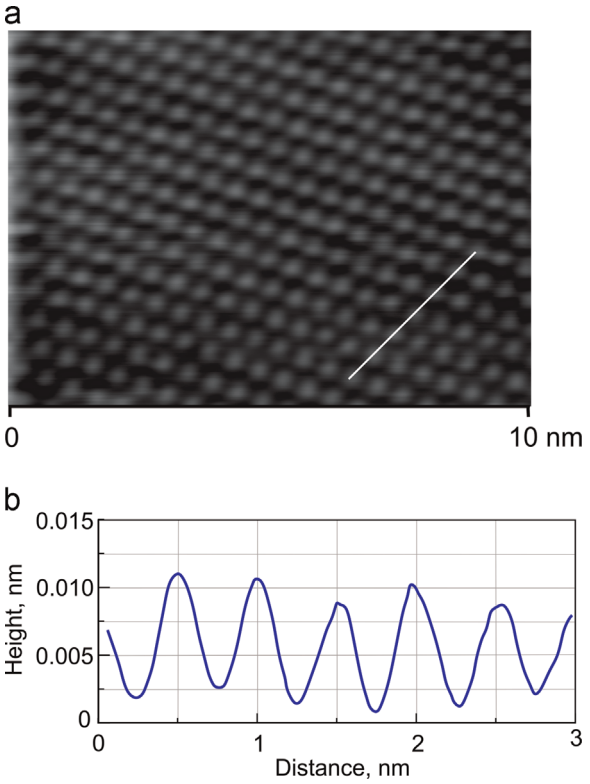

Fig. 7. The STM (a) topographic image of the Bi_2Te_3 cleaved surface acquired at the bias voltage of −1 V and (b) cross-sectional profile.

and the behavior is typical of metals [69,70]. As to the comparison with Bi_2Se_3, the refractive index of Bi_2Te_3 is noticeably lower than that of Bi_2Se_3 over the spectral range of ~250–1030 nm [63]. The extinction coefficient of Bi_2Te_3, however, is drastically higher than that of Bi_2Se_3 above 600 nm.

The survey XPS spectra recorded from the cleaved Bi_2Te_3(0001) surfaces are shown in Fig. 1S. All the spectral features recorded from the as-cleaved surface are attributed to the core-levels or Auger lines of the atoms constituting Bi_2Te_3. The presence of the low-intensity C 1s line in the survey XPS spectrum of the Bi_2Te_3(0001) surface is detected after 30 days keeping in the air. This foreign line appeared evidently due to the hydrocarbons

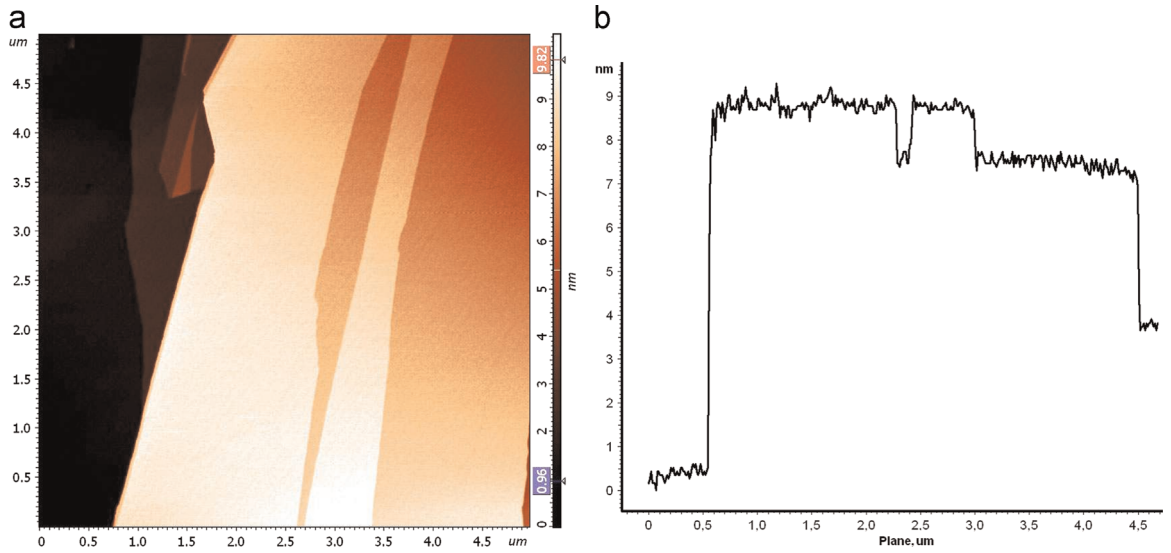

Fig. 6. The (a) AFM image and (b) related depth profile recorded for the Bi_2Te_3(0001) surface.

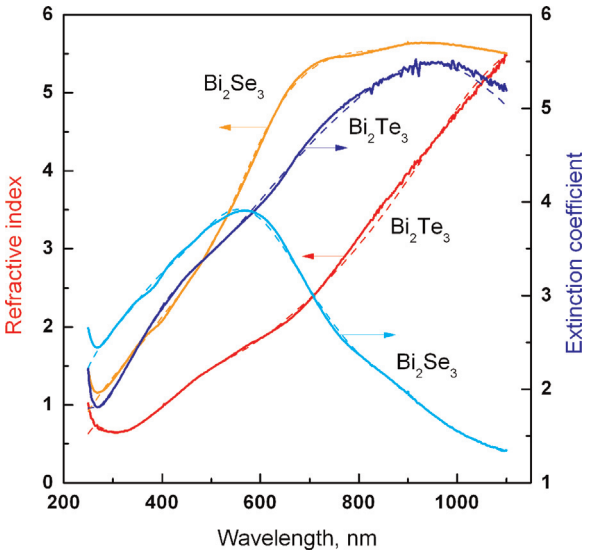

Fig. 8. The dispersion of refractive index and absorption coefficient in Bi_2Te_3 and Bi_2Se_3. Ther experimental curves and those calculated by Lorentz–Drude model are shown by continuous and interrupted lines, respectively.

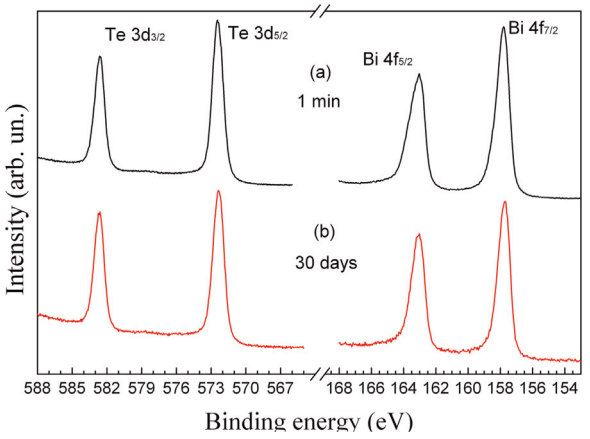

Fig. 9. The Te 3d and Bi 4f doublets, as recorded from the cleaved $Bi_2Te_3(0001)$ surface (a) just after cleavage and (b) after a 30 day exposure to the air.

adsorbed from the laboratory air. However, the $Bi_2Te_3(0001)$ oxidation is not found as it is evident from spectra shown in Fig. 2S. The detailed photoelectron spectra of Te 3d and Bi 4f doublets recorded from the $Bi_2Te_3(0001)$ surface are shown in Fig. 9. The doublets are well approximated by a combination of individual components, and that confirms unique chemical states of bismuth and tellurium in the Bi_2Te_3 just after the cleaved surface preparation and, also, after a month keeping in the laboratory air. Even after the long-time exposure to the air, no chemically-shifted oxide components were found in the photoelectron spectrum that verifies the high surface inertness to oxidation. Generally, the constituent element line parameters are in good relation with the earlier XPS measurements of Bi_2Se_3 family crystals [19,26,30,71–73]. The relative element content was estimated using the Te $3d_{5/2}$ and Bi $4f_{7/2}$ components recorded from a fresh cleaved Bi_2Te_3 surface. The measured result of Bi:Te=0.67 is in excellent agreement with the nominal composition of Bi:Te=2/3. Thus, it can be concluded that the chemically cleaned $Bi_2Te_3(0001)$ surface can be prepared by the crystal cleavage in the air environment.

The specially exposed facets of crystals have been demonstrated to show enhanced properties in various applications [74–82]. The Bi_2Se_3-type crystals, including Bi_2Te_3, possess strongly specific properties of the (0001) surface and this factor should be accounted in the microcrystal growth and TI structure preparation. The chemical interaction during epitaxy or top surface doping may be sensitive to pronounced structural anisotropy of Bi_2Te_3-based materials [1,3,9–11,13,83].

4. Conclusions

As it is shown in the present study, the high-quality Bi_2Te_3 crystals can be grown by the vertical Bridgman technique. The structural quality of the crystals is good enough for the preparation of a large area (0001) cleaved surface suitable for physical parameter measurements. The structural and chemical parameters of the surface are evaluated by RHEED, AFM, STM and XPS. The Bi_2Te_3 cleaved surface covered by atomically smooth (0001) terraces is chemically stable for a long time and, respectively, crystal cleavage can be carried out in the air atmosphere that greatly simplifies the topological insulator sample preparation and physical measurements. Further growth technology optimization, however, is topical to increase the crystal size and homogeneity needed to enlarge the atomically smooth terraces area.

Acknowledgments

This study is partly supported by the Russian Foundation for Basic Research (Grants 13-02-00706-a, 14-08-3110). The partial support from the Saint Petersburg State University (Project 11.50.202.2015) is acknowledged. The studies were partly performed using the instrumental equipment of CCU "Nanostructures". This work was supported in part by the Ministry of Education and Science of the Russian Federation (Project ID RFMEFI62114 × 0004) and RSCF (Project no. 14-22-00143). Partly, this study (research Grant no. 8.2.06.2015) was supported by the Tomsk State University Academician D.I. Mendeleev Foundation Program in 2015. VVA is partially supported by the Ministry of Education and Science of the Russian Federation.

Appendix A. Suplementary information

Supplementary data associated with this article can be found in the online version at http://dx.doi.org/10.1016/j.jssc.2015.07.031.

References

[1] Christopher J. Vineis, Ali Shakouri, Arun Majaumdar, Mercouri G. Kanatzidis, Adv. Mater. 22 (2010) 3970–3980.
[2] Paz Vaqueiro, Anthony V. Powell, J. Mater. Chem. 20 (2010) 9577–9584.
[3] M. Winkler, X. Liu, U. Schurmann, J.D. Konig, L. Kienle, W. Bensch, H. Bottner, Z. Anorg. Allg. Chem. 638 (15) (2012) 2441–2454.
[4] V.A. Kulbachinskii, V.G. Kytin, A.A. Kudryashov, P.M. Tarasov, J. Solid State Chem. 193 (2012) 47–52.
[5] B.M. Goltzman, V.A. Kudinov, I.A. Smirnov, Semiconductor Thermoelectric Materials on the Basis of Bi_2Te_3, Nauka, Moscow, 1972.
[6] J. Moore, Nat. Phys. 5 (2009) 378–380.
[7] Y. Xia, D. Qian, D. Hsieh, L. Wray, A. Pal, H. Lin, A. Bansil, D. Grauer, Y.S. Hor, R. J. Cava, M.Z. Hasan, Nat. Phys. 5 (2009) 398–402.
[8] Haijun Zhang, Chao-Xing Liu, Xiao-Liang Qi, Xi Dai, Zhong Fang, Shou-Cheng Zhang, Nat. Phys. 5 (2009) 438–442.
[9] Guang Wang, Xie-Gang Zhu, Yi-Yang Sun, Yao-Yi Li, Tong Zhang, Jing Wen, Xi Chen, Ke He, Li-Li Wang, Xu-Cun Ma, Jin-Feng Jia, Shengbai B. Zhang, Qi-Kun Xue, Adv. Mater. 23 (2011) 2929–2932.
[10] Yang Liu, Guang Bian, T. Miller, Mark Bissen, T.-C. Chiang, Phys. Rev. B 85 (2012) 195442.
[11] O.V. Yazyev, E. Kioupakis, J.E. Moore, S.G. Louie, Phys. Rev. B 85 (2012) 161101.
[12] J. Henk, M. Flieger, I.V. Maznichenko, I. Mertig, A. Ernst, E.V. Eremeev, E. V. Chulkov, Phys. Rev. Lett. 109 (7) (2012) 076801.
[13] Zuocheng Zhang, Xiao Feng, Minghua Guo, Yunbo Ou, Jinsong Zhang, Kang Li, Lili Wang, Xi Chen, Qikun Xue, Xucun Ma, Ke He, Yayu Wang, Phys. Status

Solidi (RRL) 7 (1–2) (2013) 142–144.
[14] Desheng Kong, Wenhui Dang, Judy J. Cha, Hui Li, Stefan Meister, Hailin Peng, Zhongfan Liu, Yi Cui, Nanoletters 10 (2010) 2245–2250.
[15] Guolin Hao, Xiang Qi, Yundan Liu, Zongyu Huang, Hongxing Li, Kai Huang, Jun Li, Liwen Yang, Jianxin Zhong, J. Appl. Phys. 111 (2012) 114312.
[16] Yong Wang, Faxian Xiu, Lina Cheng, Liang He, Murong Lang, Jianshi Tang, Xufeng Kou, Xinxin Yu, Xiaowei Jiang, Zhigang Chen, Jin Zou, Kang L. Wang, Nanoletters 12 (2012) 1170–1175.
[17] S. Urazhdin, D. Bilc, S.D. Mahanti, S.H. Tessmer, Theodora Kyratsi, M.G. Kanatzidis, Phys. Rev. B 69 (2004) 085313.
[18] P. Janíček, Č. Drašar, L. Beneš, P. Lošťák, Cryst. Res. Technol. 44 (5) (2009) 505–510.
[19] O.E. Tereshchenko, K.A. Kokh, V.V. Atuchin, K.N. Romanyuk, S.V. Makarenko, V.A. Golyashov, A.S. Kozhukhov, I.P. Prosvirin, A.A. Shklyaev, J. Exp. Theor. Phys. Lett. 94 (6) (2011) 465–468.
[20] N. Keawprak, S. Lao-ubol, C. Eamchotchawalit, Z.M. Sun, J. Alloy. Compd. 509 (2011) 9296–9301.
[21] Han Liu, Peide D. Ye, Appl. Phys. Lett. 99 (2011) 052108.
[22] V. Chis, I.Yu Sklyadneva, K.A. Kokh, V.A. Volodin, O.E. Tereshchenko, E.V. Chulkov, Phys. Rev. B 86 (2012) 174304.
[23] D. West, Y.Y. Sun, S.B. Zhang, T. Zhang, Xucun Ma, P. Cheng, Y.Y. Zhang, X. Chen, J.F. Jia, Q.K. Xue, Phys. Rev. B 85 (2012) 081305(R).
[24] K.A. Kokh, S.V. Makarenko, V.A. Golyashov, O.A. Shegai, O.E. Tereshchenko, CrystEngComm 16 (2014) 581–584.
[25] M. Ye, S.V. Eremeev, K. Kuroda, E.E. Krasovskii, E.V. Chulkov, Y. Takeda, Y. Saitoh, K. Okamoto, S.Y. Zhu, K. Miyamoto, M. Arita, M. Nakatake, T. Okuda, Y. Ueda, K. Shimada, H. Namatame, M. Taniguchi, A. Kimura, Phys. Rev. B 85 (2012) 205317.
[26] V.A. Golyashov, K.A. Kokh, S.V. Makarenko, K.N. Romanyuk, I.P. Prosvirin, A.V. Kalinkin, O.E. Tereshchenko, A.S. Kozhukhov, D.V. Sheglov, S.V. Eremeev, S.D. Borisova, E.V. Chulkov, J. Appl. Phys. 112 (2012) 113702.
[27] Qi Zhang, Jun Su, Xianghui Zhang, Jian Li, Aiqing Zhang, Yihua Gao, J. Alloy. Compd. 545 (2012) 105–110.
[28] Heon-Jung Kim, Ki-Seok Kim, J.-F. Wang, V.A. Kulbachinskii, K. Ogawa, M. Sasaki, A. Ohnishi, M. Kitaura, Y.-Y. Wu, L. Li, I. Yamamoto, J. Azuma, M. Kamada, V. Dobrosavijević, Phys. Rev. Lett. 110 (2013) 136601.
[29] M.R. Scholz, J. Sánchez-Barriga, D. Marchenko, A. Varykhalov, A. Volykhov, L. V. Yashina, O. Rader, Phys. Status Solidi (RRL) 7 (1–2) (2013) 139–141.
[30] A.M. Shikin, I.I. Klimovskikh, S.V. Eremeev, A.A. Rybkina, M.V. Rusinova, A. G. Rybkin, E.V. Zhizhin, J. Sánchez-Barriga, A. Varykhalov, I.P. Rusinov, E. V. Chulkov, K.A. Kokh, V.A. Golyashov, V. Kamyshlov, O.E. Tereshchenko, Phys. Rev. B 89 (2014) 125416.
[31] G.H. Winton, L. Faraone, R. Lamb, J. Vaccum Sci. Technol. 12 (1) (1994) 35–43.
[32] V.V. Vasilyev, N.I. Zakharyash, V.G. Kesler, I.O. Parm, A.P. Soloviev, Semiconductors 35 (2) (2001) 196–198.
[33] O.A. Balitskii, W. Jaegermann, Mater. Chem. Phys. 97 (2006) 98–101.
[34] Y. Yang, S.C. Kung, D.K. Taggart, C. Xiang, F. Yang, M.A. Brown, A.G. Güell, T.J. Kruse, J.C. Hemminger, R.M. Penner, Nanoletters 8 (8) (2008) 2447–2451.
[35] D. Telesca, Y. Nie, J.I. Budnick, B.O. Wells, B. Sinkovic, Phys. Rev. B 85 (2012) 214517.
[36] E.J. Menke, M.A. Brown, Q. Li, J.C. Hemminger, R.M. Penner, Langmuir 22 (2006) 10564–10574.
[37] Bo Zhou, Yu Zhao, Lin Pu, Jun-Jie Zhu, Mater. Chem. Phys. 96 (2006) 192–196.
[38] Yixin Zhao, Clemens Burda, ACS Appl. Mater. Interfaces 1 (6) (2009) 1259–1263.
[39] Jang-Jung Kim, Sook-Hyun Kim, Seung-Wook Suh, Dong-Uk Choe, Byung-Ki Park, Jae-Rock Lee, Young-Seak Lee, J. Cryst. Growth 312 (2010) 3410–3415.
[40] T.P. Debies, J.W. Rabalais, Chem. Phys. 20 (2) (1977) 277–283.
[41] H. Bando, K. Koizumi, Y. Oikawa, K. Daikohara, V.A. Kulbachinskii, H. Ozaki, J. Phys.: Condens. Matter 12 (2000) 5607–5616.
[42] F. Körber, U. Haschimoto, Z. Anorg. Allg. Chem. 188 (1) (1930) 114–126.
[43] N.Kh Abrikosov, V.F. Bankina, Zh. Neorg. Khim. 3 (3) (1958) 659–667.
[44] C.C. Liu, J.C. Angus, J. Electrochem. Soc. 116 (8) (1969) 1054–1060.
[45] V.V. Atuchin, T.A. Gavrilova, K.A. Kokh, N.V. Kuratieva, N.V. Pervukhina, N. V. Surovtsev, Solid State Commun. 152 (13) (2012) 1119–1122.
[46] Tadashi C. Ozawa, Sung J. Kang, J. Appl. Cryst. 37 (2004) 679.
[47] E.Ya Atabaeva, E.S. Itskevich, S.A. Mashkov, S.V. Popova, L.F. Vereshchagin, Fiz. Tverd. Tela 10 (1) (1968) 62–65.
[48] H. Okamoto, J. Phase Equilib. 15 (1994) 195–201.
[49] Yu.V. Shevtsov, N.F. Beizel, Inorg. Mater. 47 (2011) 139–142.
[50] K.A. Kokh, B.G. Nenashev, A.E. Kokh, G.Yu Shvedenkov, J. Cryst. Growth 275 (2005) e2129–e2134.
[51] K.A. Kokh, V.N. Popov, A.E. Kokh, B.A. Krasin, A.I. Nepomnyaschikh, J. Cryst. Growth 303 (2007) 253–257.
[52] P. Janček, Č. Drašar, L. Beneš, P. Lošťák, Cryst. Res. Technol. 44 (5) (2009) 505–510.
[53] S.Yu. Sarkisov, V.V. Atuchin, T.A. Gavrilova, V.N. Kruchinin, S.A. Bereznaya, Z.V. Korotchenko, O.P. Tolbanov, A.I. Chernyshev, Russ. Phys. J. 53 (4) (2010) 346–352.
[54] K.A. Kokh, Yu.M. Andreev, V.A. Svetlichnyi, G.V. Lanskii, A.E. Kokh, Cryst. Res. Technol. 46 (4) (2011) 327–330.
[55] K.A. Kokh, V.V. Atuchin, T.A. Gavrilova, A. Kozhukhov, E.A. Maximovskiy, L.D. Pokrovsky, A.G. Tsygankova, A.I. Saprykin, J. Microsc. 256 (3) (2014) 208–212.
[56] V.V. Atuchin, N.V. Ivannikova, A.I. Komonov, N.V. Kuratieva, I.D. Loshkarev, N.V. Pervukhina, L.D. Pokrovsky, V.N. Shlegel, CrystEngComm 17 (24) (2015) 4512–4516.
[57] Yu.M. Andreev, V.V. Atuchin, G.V. Lanskii, A.N. Morozov, L.D. Pokrovsky, S.Yu. Sarkisov, O.V. Voevodina, Mater. Sci. Eng. B 128 (2006) 205–210.
[58] C.V. Ramana, V.V. Atuchin, U. Becker, R.C. Ewing, L.I. Isaenko, O.Yu. Khyzhun, A.A. Merkulov, L.D. Pokrovsky, A.K. Sinelnichenko, S.A. Zhurkov, J. Phys. Chem. C 111 (2007) 2702–2708.
[59] A.A. Shklyaev, V.I. Vdovin, V.A. Volodin, D.V. Gulyaev, A.S. Kozhukhov, M. Sakuraba, J. Murota, Thin Solid Films 579 (2015) 131–135.
[60] A.A. Shklyaev, K.N. Romanyuk, S.S. Kosolobov, Surf. Sci. 625 (2014) 50–56.
[61] E.J. Rubio, V.V. Atuchin, V.N. Kruchinin, L.D. Pokrovsky, I.P. Prosvirin, C.V. Ramana, J. Phys. Chem. C 118 (2014) 13644–13651.
[62] S.V. Rykhlitski, E.V. Spesivtsev, V.A. Shvets, V.Yu Prokopiev, Instrum. Exp. Tech. (2) (2007) 160–161.
[63] V.V. Atuchin, E.N. Galashov, O.Yu. Khyzhun, A.S. Kozhukhov, L.D. Pokrovsky, V.N. Shlegel, Cryst. Growth Des. 11 (2011) 2479–2484.
[64] E.N. Galashov, V.V. Atuchin, A.S. Kozhukhov, L.D. Pokrovsky, V.N. Shlegel, J. Cryst. Growth 401 (2014) 156–159.
[65] V.V. Atuchin, E.N. Galashov, O.Y. Khyzhun, V.L. Bekenev, L.D. Pokrovsky, Yu. A. Borovlev, V.N. Zhdankov, J. Solid State Chem. (2015), http://dx.doi.org/10.1016/j.jssc.2015.05.017.
[66] V.V. Atuchin, V.A. Golyashov, K.A. Kokh, I.V. Korolkov, A.S. Kozhukhov, V. N. Kruchinin, S.V. Makarenko, L.D. Pokrovsky, I.P. Prosvirin, K.N. Romanyuk, O. E. Tereshchenko, Cryst. Growth Des. 11 (2011) 5507–5514.
[67] D. Barton, F.K. Urban III, Thin Solid Films 516 (2007) 119–127.
[68] V.V. Atuchin, Z.S. Lin, L.I. Isaenko, V.G. Kesler, V.N. Kruchinin, S.I. Lobanov, J. Phys.: Condens. Matter 21 (2009) 455502.
[69] E.D. Palik, Handbook of Optical Constants of Solids, Academic Press, New York/Orlando, 1985.
[70] V.V. Atuchin, T.I. Grigorieva, L.D. Pokrovsky, V.N. Kruchinin, D.V. Lychagin, C.V. Ramana, Phys. Lett. B 26 (5) (2012) 1150029.
[71] L.V. Yashina, J. Sánchez-Barriga, M.R. Scholz, A.A. Volykhov, A.P. Sirotina, V.S. Neudachina, M.E. Tamm, A. Varykhalov, D. Marchenko, G. Springholz, G. Bauer, A. Knop-Gericke, O. Rader, ACS Nano 7 (6) (2013) 5181–5191.
[72] A.S. Hewitt, J.G. Wang, J. Botlersdorf, P.A. Maggard, J. Vaccum Sci. Technol. B 32 (4) (2014) 04E103.
[73] M.T. Edmonds, J.T. Hellerstedt, A. Tadich, A. Schenk, K.M. O'Donnell, J. Tosado, N.P. Butch, P. Syers, J. Paglione, M.S. Fuhrer, J. Phys. Chem. C 118 (35) (2014) 20413–20419.
[74] C.V. Ramana, V.V. Atuchin, I.B. Troitskaia, S.A. Gromilov, V.G. Kostrovsky, G.B. Saupe, Solid State Commun. 149 (2009) 6–9.
[75] Xianjun Du, Dengsong Zhang, Liyi Shi, Ruihua Gao, Jianping Zhang, J. Phys. Chem. C 116 (2012) 10009–10016.
[76] Yadong Kebin Zhou, Angew. Chem. Int. Ed. 51 (2012) 602–613.
[77] G.S. Zakharova, C. Taschner, T. Kolb, C. Jahne, A. Leonhardt, B. Buchner, R. Klingeler, Dalton Trans. 42 (14) (2013) 4897–4902.
[78] Ruihua Gao, Dengsong Zhang, Phornphimon Maitarad, Liyi Shi, Thanyada Rungrotmongkol, Hongrui Li, Jianping Zhang, Weiguo Cao, J. Phys. Chem. C 117 (2013) 10502–10511.
[79] E.V. Alekseev, O. Felbinger, Shijun Wu, T. Malcherek, W. Depmeier, G. Modolo, T.M. Gesing, S.V. Krivovichev, E.V. Suleimanov, T.A. Gavrilova, L.D. Pokrovsky, A.M. Pugachev, N.V. Surovtsev, V.V. Atuchin, J. Solid State Chem. 204 (2013) 59–63.
[80] T. Bathon, P. Sessi, K.A. Kokh, O.E. Tereshchenko, M. Bode, Nanoletters 15 (4) (2015) 2442–2447.
[81] S. Yang., Y. Liu, W. Jin, Y. Qi, G.S. Zakharova, W. Chen, Ferroelectrics 477 (1) (2015) 112–120.
[82] G. Landolt, S.V. Eremeev, O.E. Tereshchenko, S. Muff, K.A. Kokh, J. Osterwalder, E.V. Chulkov, J.H. Dil, Phys. Rev. B 91 (2015) 081201.
[83] O. Caha, A. Dubroka, J. Humlíček, V. Holý, H. Steiner, M. Ul-Hassan, J. Sánchez-Barriga, O. Rader, T.N. Stanislavchuk, A.A. Sirenko, G. Bauer, G. Springholz, Cryst. Growth Des. 13 (8) (2013) 3365–3373.

Please cite this article as: V.V. Atuchin, et al., J. Solid State Chem. (2015), http://dx.doi.org/10.1016/j.jssc.2015.07.031